Journal of the Ceramic Society of Japan 119 [2] 125-128 2011 **Paper**

Carbon nanotubes formation from Fe/Ni/Mg by camphor oil decomposition

A. A. AZIRA,[*,**,†] **A. B. SURIANI**[*,**] **and M. RUSOP**[*,***]

[*]**NANO-SciTech Centre (NST), Institute of Science, Universiti Teknologi MARA, 40450 Shah Alam, Selangor, Malaysia**
[**]**Faculty of Applied Sciences, Universiti Teknologi MARA, 40450 Shah Alam, Selangor, Malaysia**
[***]**NANO-ElecTronic Centre (NET), Faculty of Electrical Engineering, Universiti Teknologi MARA,**
40450 Shah Alam, Selangor, Malaysia

In this study, carbon nanotubes were formed from camphor oil decomposition on Fe/Ni/Mg catalysts at 650°C by fluidized floating catalyst method. X-ray diffraction (XRD) was used to examine the characteristics of carbon nanotubes. The carbon nanotubes were also examined both by FESEM and Raman spectroscopy to define their appearance and structure which revealed that dense bundle of mixed multi-walled and single-walled carbon nanotubes. The diameters of the single-walled carbon nanotubes were estimated to be around 0.86–2.31 nm. Little amount of carbon nanotubes were found on the Fe/Ni/Mg catalyst surface at 550°C; while a significant amount of carbon nanotubes were observed at 650°C. According to the XRD spectrum, there was carbon and graphite present in the deposited samples. Raman spectroscopy revealed two peaks at 1347–1357 cm^{-1} (D band, disorder mode, amorphous carbon) and 1572 cm^{-1} (G band, graphite sp^2 structure). FESEM results indicated the Fe/Ni/Mg could catalyze the camphor oil decomposition to form carbon nanotubes even at a lower temperature.

Key-words : carbon nanotubes, modified fluidized floating catalyst method, catalyst

[Received September 22, 2010; Accepted December 8, 2010]

1. Introduction

Fluidized bed reactors are widely applied for several industrial purposes, such as different types of chemical reactors, fluid catalytic cracking, fluidized bed combustion, fluidized bed biofilter or applying a coating on solid items.[1)] Fluidized bed reactors afford excellent gas–solid contacting and particle mixing, facilitate the control of highly exothermal reactions, and provide good gas-to-particle and bed-to-wall. Recently, fluidized bed reactors with supported nano-metal catalysts were found to be equally effective for mass production of carbon nanotubes (CNTs).[1)–7)] In the mass production of CNTs, fluidized bed chemical vapor deposition (FBCVD) techniques offer numerous advantages over fixed beds and floating catalyst thanks to the technology robustness, flexibility and high productivity.[8)–12)] Moreover, the FBCVD is easily scaled-up and can be operated continuously which is important for cost-effective large-scale production of CNTs as being employed in this study.

Basically, fluidization provides higher space velocity which leads to efficient gas–solid contact, and hence high mass and heat transfer. In accordance with that high process yield, product homogeneity, purity and selectivity are attained.[8)–10)] Moreover, FBCVD is a flexible process in terms of operating conditions as parameters like gas mixture and temperature can be finely tuned according to the definition of the desired product.[10),13)] Furthermore, available space for growing CNTs and their resistance times can be controlled accurately and the activity of the catalyst is utilized sufficiently[9),10)] which favors the selective mass production of CNTs with uniform properties.

This study investigated the characteristics of camphor oil decomposition on Fe/Ni/Mg trimetallic catalyst and formation of CNTs by FBCVD on the effect of the deposition temperature as an advancement of previous study.[14),15)] In addition, FESEM, Raman spectroscopy, and XRD were used to examine the physiochemical properties of CNTs. The characteristics of the CNTs formed from Fe/Ni/Mg were compared. Furthermore, the temperature effect of the CNTs formation was also investigated.

2. Experimental

The growth of CNTs was carried out in a tubular furnace with a horizontal quartz tube at atmospheric pressure using FBCVD. First, carrier gas (argon) was flushed for about 10 min before the furnace was turned on to remove the surrounding air and to create an inert atmosphere. Then, the precursor (camphor oil) and catalyst (Fe/Ni/Mg) mixtures were placed together in a quartz boat and pushed into the center of the quartz tube. Then the quartz tube was heated in Ar ambient with a flow rate of 50 standard cubic centimeter (sccm) to flush out any presence of other gases especially oxygen. When the temperature of the furnace was rapidly increased to the desired deposition temperature, CNTs was found to be deposited in the quartz boat. Annealing process was then carried out by maintaining the temperature for a further period of 30 min. Finally, the quartz tube was cooled down to room temperature in Ar ambient with a flow rate of 50 sccm. The carbon deposited materials formed were removed from the quartz boat. The carbon materials were characterized by FESEM (JSEM 6700F), microraman spectroscopy (Horiba Jobin Yvon-DU420A-OE-325) and XRD (Rigaku D-Max 2000).

[†] Corresponding author: A. A. Azira; E-mail: aziraaziz@yahoo.com

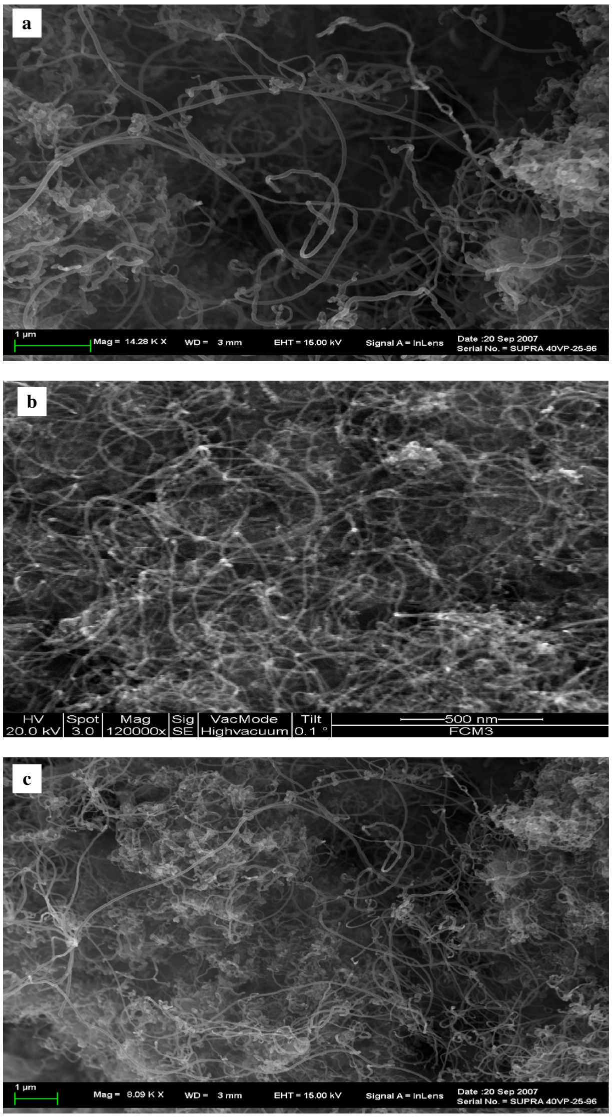

Fig. 1. (Color online) FESEM images of CNTs deposited at (a) 550°C, (b) 650°C and (c) 750°C.

3. Results and discussion

3.1 FESEM analyses

Figure 1 shows FESEM micrographs of carbon filaments on the Fe/Ni/Mg catalysts. Figure 1(a) displays little CNTs were observed at 550°C on the catalyst surface. Figure 1(b) shows the CNTs formation at 650°C displays huge and more CNTs formation at 550°C with diameter around 30–40 nm. Figure 1(c) exhibits lesser CNTs were observed at 750°C compared to CNTs formation at 650°C with diameter around 23–25 nm. The diameter of the CNTs in Fig. 1(b) ranged around 11–15 nm. According to the figures, Fe/Ni/Mg catalyzed the camphor oil decomposition and formed high yield of CNTs even at a low deposition temperature as shown in **Fig. 2**.

Therefore, CNTs deposited at 650°C can be considered as optimum temperature due to high yield and uniform growth distribution of CNTs compared to other deposition temperature. The variation in concentration of the catalyst varies the quantity of CNTs growth. Hence, in this study we fixed the concentration of catalyst with the catalyst ratio 1:1:1 in all the samples. Materials with capability of decomposing hydrocarbon and CNTs formation are employed as for the formation of the tubes. However, it has been found that only the hydrocarbon molecules decomposing ability of catalyst could not be accounted for the CNT formation. These results emphasize that careful selection of the catalyst concentration is a dominating factor in synthesis of CNTs. Mixing transition metals in the form of nanoparticles are considered as the most effective catalysts and will help to reduced the deposition temperature. The peculiar ability of the transition metals to promote CNT growth is strongly related to these factors: (a) catalytic activity for decomposition of volatile carbon compounds, (b) ability of metastable carbides formation, and (c) diffusion of carbon through and over the metallic particles. The formation process for CNTs growth utilizes heterogeneous catalysts, which are the catalytically active metal particles, typically with a diameter of 1–10 nm, anchored on a high surface inert area.

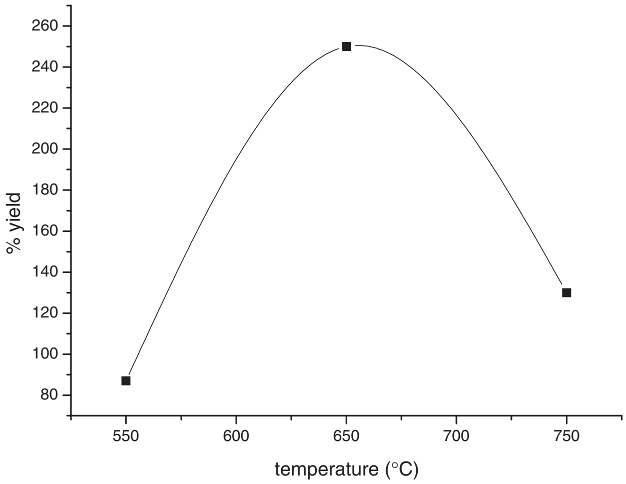

Fig. 2. % of CNTs yield versus deposition temperature.

3.2 Raman spectroscopy

The micro-Raman spectra of as-grown CNTs are shown in **Figs.** 3(a)–3(c). The most noticeable features in the first-order Raman spectra were detected for CNTs deposited at 550, 650 and 750°C at around 1572 cm^{-1} (G peak) and 1347 cm^{-1} (D peak). The G peak is assigned to the Raman-allowed C-C phonon mode (E_{2g} band) of graphite lattice and D peak represent the disorder-induced phonon mode (A_{1g} band).[16] The slight and significant shift of D and G peak positions were noted; this attributed to the structural dissimilarity of the nanotubes growth. The G peak intensity is also seen prominent at CNTs deposited at 650°C. This indicates better graphitization of CNTs produced at 650°C compared to 550°C and 650°C. As for I_D/I_G ratio which measures the quality of the nanotubes, the I_D/I_G value was found to be 0.82, 0.31 and 0.42 for CNTs deposited at 550, 650 and 750°C, respectively. This shows that the defect level is higher at lower deposition temperature than higher deposition temperature which is in good agreement with FESEM analysis. The peaks position and the I_D/I_G ratio for both samples are summarized in **Table 1**.

Figure 4 illustrates lower frequency radial breathing mode (RBM) peaks for the CNTs. There were 4 obvious peaks detected at 107, 109, 190 and faint peak at 287 cm^{-1}. However there are no lower frequencies detected for CNTs deposited at 550°C. The presence of this peaks suggested that single wall nanotubes (SWNTs) exist in the deposited CNTs. The diameter, *d* of

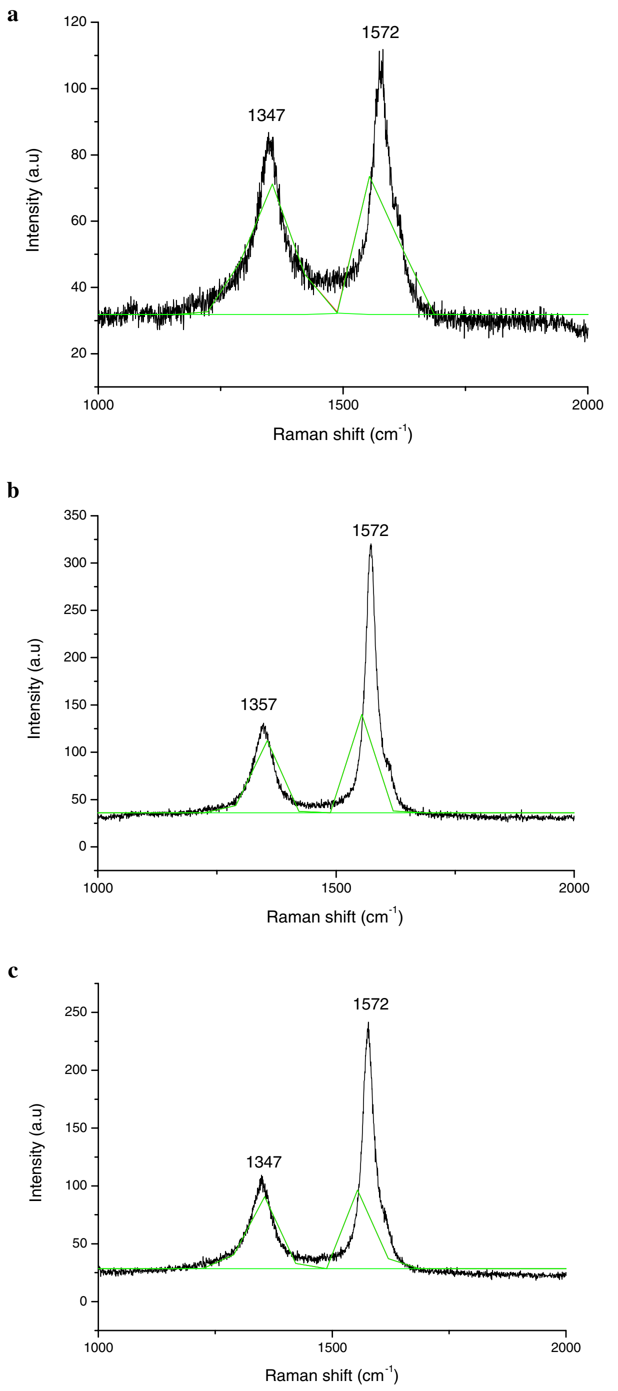

Fig. 3. (Color online) Typical Raman of CNTs deposited at (a) 550°C, (b) 650°C and (c) 750°C.

SWNTs can be calculated from RBM peak frequency $\omega\,\mathrm{cm}^{-1}$ using the equation $d\ (\mathrm{nm}) = 248\ (\mathrm{cm}^{-1}\,\mathrm{nm})/\omega\ (\mathrm{cm}^{-1})$.[17] According to the stated equation, the RBM frequency of 107, 109, 190 and 287 cm^{-1} correspond to the SWNTs with diameter of 2.31, 2.27, 1.30 and 0.86 nm respectively.

Table 1. Raman peak position and D & G intensity ratios for CNTs at different deposition temperature

Deposition temperature (°C)	D band (cm^{-1})	G band (cm^{-1})	Intensity ratio (I_D/I_G)
550	1347.0	1572.0	0.82
650	1357.0	1572.0	0.31
750	1347.0	1572.0	0.42

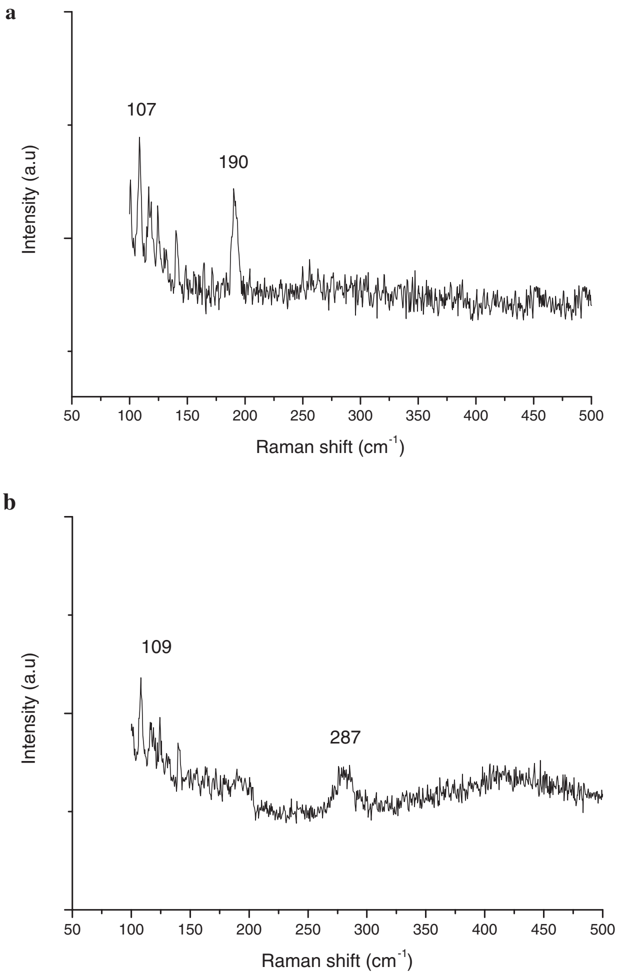

Fig. 4. The multiple low frequency peaks associated with radial breathing mode (RBM) for CNTs deposited at (a) 650°C and (b) 750°C.

3.3 X-ray diffraction

The XRD patterns for CNTs at a function of different catalyst are shown in **Fig. 5** in order to investigate the samples ordering and to determine the degree of graphitic character. The characteristic peaks of CNTs are mostly detected and marked in the figure and the profile is typically of well-crystallized materials as observed in FESEM images. From the XRD pattern, the peaks can be indexed to (002), (100), (101) and (004) hexagonal graphite (JCPDS, 41-1487), respectively.[18] The strong and sharp peaks suggest that the as-prepared products are well crystallized and no obvious impurity peak in the pattern. The characteristic intense graphite peaks at (002) at $2\theta \approx 26°$ is seen in all cases. Other significant observations are peaks at 40, and 54°. The 40° peak corresponds to overlapping (100) and (101) reflection while 54° corresponds to (004) reflection. From the best of our knowledge, the shift in the spectra might be due some of the catalyst nanoparticle will be diffuse into the carbon lattice during the growth of nanotubes. Through the catalyst ion incorporation in the graphene lattice which will cause the shift in the spectra. This will probably cause in-plane lattice expansion of the graphene-plane of CNT that contribute a slight shift from 40 to 43° due to the above mentioned reasons. The presence of these

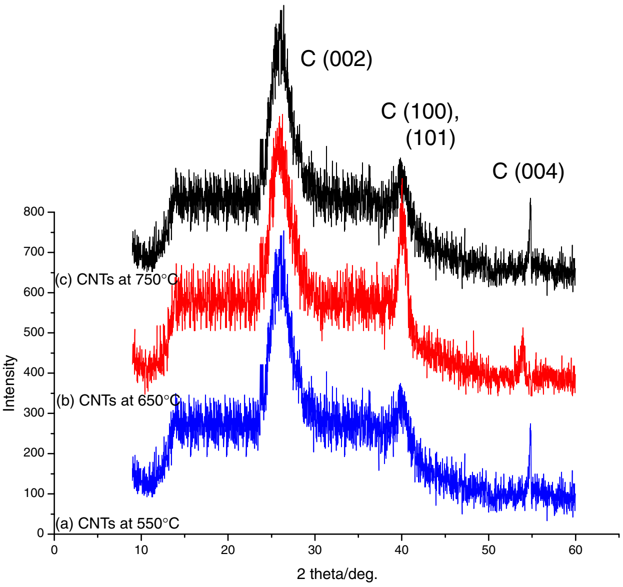

Fig. 5. (Color online) XRD spectra of CNTs at different deposition temperature.

peaks is also indicative of improved in-plane (cylindrical layer) and interlayer graphitic structure.[19] High intensity noted from Fig. 5(b) CNTs deposited at 650°C due to high graphitization in the structure compared to other deposition temperature.

4. Conclusion

The synthesis of CNTs has been demonstrated using camphor oil as the carbon source and Fe/Ni/Mg nanoparticles as the catalyst by FBCVD. As speculated, by applying this method with trimetallic catalyst might contribute to deposit good quality of CNTs with high yield even at low deposition temperature. The technique was capable of producing CNTs with high yield and purity with minimal amorphous carbon content. However, better graphitization and uniform growth deposition were formed at 650°C. At 550°C, CNTs growth was detected but at 650°C the samples contain mixture of MWNTs and SWNTs, respectively. However, at 750°C CNTs growth gave thicker nanotubes because the diameter increases gradually with increasing temperature due to the agglomeration of the catalyst metal oxides particles. Raman spectroscopy revealed that I_D/I_G is lower for CNTs deposited at 650°C (0.31) which explained low defect in the structure compared to CNTs deposited at 550 and 750°C (0.82 and 0.42). XRD spectra of all the samples shows dominant peaks at (002), (100), (101) and (004) which indicated improved in-plane (cylindrical layer) and interlayer graphitic of the CNTs. The peaks suggest that the CNTs are well crystallized and no obvious impurity peak in the pattern. Furthermore, this technique can be effectively adopted in industry for the synthesis of bulk CNTs. The simplicity of incorporating the optimum catalyst material into the carbon source material and the economy of utilizing a readily available, renewable green source renders this technique a significant potential for large scale commercial for production of CNTs.

Acknowledgement The authors would like to thank NANO-SciTech Centre and Faculty of Applied Sciences, UiTM, and MOSTI for the facilities and financial support on this project.

References

1) C. Vahlas, B. Caussat, Ph. Serp and G. N. Angelopoulos, *Mater. Sci. Eng., R*, 53, 1–72 (2006).
2) Ph. Venegonia, R. Serp, R. Feurer and Y. Kihn, *Carbon*, 40, 1799–1807 (2002).
3) Y. Liu, W. Qian, Q. Zhang, G. Ning, G. Luo, Y. Wang, D. Wang and F. Wei, *Chem. Eng. Technol.*, 32, 73–79 (2009).
4) V. N. Parmon, G. G. Kuvshinov, V. A. Sadykov and V. A. Sobyanin, *Stud. Surf. Sci. Catal.*, 119, 677–684 (1998).
5) Q. Weizhong, L. Tang, W. Zhanwen, W. Fei, L. Zhifei, L. Guohuaa and L. Yongdan, *Appl. Catal., A*, 260, 223–228 (2004).
6) S. Y. Son, D. H. Lee, S. D. Kim and S. W. Sung, *J. Ind. Eng. Chem.*, 13, 257–264 (2007).
7) Y. Wang, F. Wei, G. Gu and H. Yu, *Physica B*, 323, 327–329 (2002).
8) R. Philippe, Ph. Serp, Ph. Kalck, Y. Kihn, S. Bordère, D. Plee, P. Gaillard, D. Bernard and B. Caussat, *AIChE J.*, 55, 450–464 (2009).
9) W. Z. Qian, W. Fei, W. Zhanwen, L. Tang, Y. Hao, L. Guohua and X. Lan, *AIChE J.*, 49, 619–625 (2003).
10) C. T. Hsieh, Y. T. Lin, W. Y. Chen and J. L. Wei, *Powder Technol.*, 192, 16–22 (2009).
11) N. Shah, Sh. Ma, Y. Wang and G. P. Huffman, *Int. J. Hydrogen Energy*, 32, 3315–3319 (2007).
12) C. H. See and A. T. Harris, *AIChE J.*, 54, 657–664 (2008).
13) R. Philippe, A. Morançais, M. Corrias, B. Caussat, Y. Kihn, P. Kalck, D. Plee, P. Gaillard, D. Bernard and Ph. Serp, *Chem. Vap. Deposition*, 13, 447–457 (2007).
14) A. A. Azira, N. F. A. Zainal, S. F. Nik, F. Mohamad, T. I. T. Kudin, T. Soga, S. Abdullah and M. Rusop, *Mater. Res. Innovations*, 13, 182–184 (2009).
15) A. A. Azira, N. F. A. Zainal, S. F. Nik, T. Soga, S. Abdullah and M. Rusop, *Int. J. Nanosci.*, 8, 351–357 (2009).
16) P. Ghosh, T. Soga, K. Ghosh, R. A. Afre, T. Jimbo and Y. Ando, *J. Non-Cryst. Solids*, 354, 4101–4106 (2008).
17) R. Saito, G. Dresselhaus and M. S. Dresselhaus, *Phys. Rev. B*, 61, 2981–2990 (2000).
18) C. Tao, F. Zhiyong, Z. Guifu, H. Qixiu, H. Biau, Y. Xiaozhi and Z. Youjin, *Bull. Mater. Sci.*, 29, 701–704 (2006).
19) W. Z. Zhu, D. E. Miser, W. G. Chan and M. R. Hajaligol, *Mater. Chem. Phys.*, 82, 638–647 (2003).